Case Studies in Thermal Engineering 43 (2023) 102779

Contents lists available at ScienceDirect

Case Studies in Thermal Engineering

journal homepage: www.elsevier.com/locate/csite

Effect of surfaces roughness of a staggered tube bank in cross flow with air on heat transfer and pressure drop

Mohamed A. Karali[a,*], Bandar Awadh Almohammadi[b], Abdullah S. Bin Mahfouz[c], Mostafa A.H. Abdelmohimen[d,e], El-Awady Attia[f], H.A. Refaey[b,e]

[a] Department of Mechanical Engineering, Faculty of Engineering and Technology, Future University in Egypt, 90 St, New Cairo, Egypt
[b] Department of Mechanical Engineering, College of Engineering at Yanbu, Taibah University, Yanbu Al-Bahr, 41911, Saudi Arabia
[c] Department of Chemical Engineering, University of Jeddah, Asfan Road, Jeddah 23890, Saudi Arabia
[d] Department of Mechanical Engineering, King Khalid University, P.O. Box 9004, Abha, 61413, Saudi Arabia
[e] Department of Mechanical Engineering, Faculty of Engineering at Shoubra, Benha University, 11629, Cairo, Egypt
[f] Industrial Engineering Department, College of Engineering, Prince Sattam Bin Abdulaziz University, Al-Kharj, 11942, Saudi Arabia

ARTICLE INFO

Keywords:
Surface roughness
Banks of tubes
Staggered arrangement
Splitter plates
Heat transfer
Pressure drop

ABSTRACT

Many options are devoted to enhancing heat transfer alongside lowering the pressure drop inside the tube banks in cross flow with air. Among these, is attaching splitter plates (SPs) to the trailing edges of the tubes as extended surfaces. That already proved from literature its effective use. Another proposed option is to increase the surface's roughness, with limited available data from literature. Thus, the present research was established to study the effect of using different surface roughness of a staggered tube-bank in cross flow with air on heat transferred and pressure drop besides the comparison with installing SPs. To this aim, a full 3D CFD model is developed to study the two mentioned options without any symmetrical boundary conditions. The study extended to include the effect of Re_{max} changes from 5000 to 100,000. While three surface relative roughness; $k_s/D = 0$ (smooth), $k_s/D = 0.01$, and $k_s/D = 0.02$ are investigated. The results confirmed that increasing heat transfer surface roughness helps to augment the total heat transferred. While a limited pressure drop increase is reported compared to installing SPs. Combining both; increasing surface roughness, and, adding SPs, led to multiplying the total heat transfer rate.

Nomenclature

A	area, m^2
$C1-C3$	constants in Eq. 6
D	tube outer diameter, mm
G_b	rate of turbulence kinetic energy related to buoyancy, J/kg.s
G_k	rate of turbulence kinetic energy related to mean velocity gradients, J/kg.s
H	fluid duct height, mm
h	convection heat transfer coefficient, $W/m^2.K$
k	turbulent kinetic energy, J/kg
K	fluid thermal conductivity, W/m.K

* Corresponding author.
E-mail addresses: mohamedkarali@yahoo.com, mkarali@fue.edu.eg (M.A. Karali).

https://doi.org/10.1016/j.csite.2023.102779
Received 17 August 2022; Received in revised form 19 January 2023; Accepted 26 January 2023
Available online 30 January 2023

k_s	surface roughness height, mm
k_s/D	surface relative roughness, dimensionless
L	splitter plate length, mm
$\dot{m}$	total mass flow rate, kg/s
N	number of tubes
p	static pressure, Pa
Q	total heat transfer rate, W
S	pitch, mm
t	splitter plate thickness, mm
t	time, sec
T	temperature, K
u	velocity vector, m/s
u'	fluctuating velocity, m/s
v	velocity, m/s
W	fluid duct width, mm
y^+	Mesh specification near the wall, dimensionless

Abbreviations

avg	average
CFD	computational fluid dynamics
LES	large eddy simulations
max	maximum
RANS	Reynolds average Naveir-Stokes
TKE	turbulent kinetic energy

Dimensionless groups

Nu	Nusselt number
Pr	Prandtl number
Re	Reynolds number

Subscripts

a	air
avg	average
D	diagonal
i	inlet
L	longitudinal
lm	logarithmic mean
max	maximum
o	outlet
s	surface
SP	splitter plate
T	transversal
t	turbulent
∞	upstream fluid

Greek letters

ρ	fluid density, kg/m^3
ε	dissipation rate, m^2/s^3
μ	fluid dynamic viscosity, Pa.s
Δ	difference
δ_{ij}	Kronecker delta, dimensionless

1. Introduction

There are many options that introduced by literature for heat transfer increasing associated to tube bank in cross flow with air [1]. One method of enhancement can be by roughening the heat transfer surfaces as it enhances the turbulence. The surface roughness of a circular tube can be identified by: the surface roughness height, k_s or the surface relative roughness, k_s/D. Where k_s is the equivalent sand grain roughness height in mm or μm, and D is the tube outer diameter. Usually, increases the surface roughness resulting in increasing the drag coefficient of turbulent flow. While, bodies, like a sphere, and circular cylinder, growing the surface's roughness might reduce the drag coefficient [2]. The roughness conditions determine the essential Reynolds number as well as the drag coefficient. The literature introduces many surface roughening procedures. The most used techniques involved the following: sandpaper [3–6], sand-grain [7], arrays of rods [8,9], and regular arrangements of pyramids [10–13]. The effect of roughness on thermal boundary layer and heat transfer coefficient of air flow around a circular cylinder has been experimentally investigated in several works [4,8–11,13,14], and numerical studies [15–18]. However, available numerical works are adopted to investigate the effect of roughness on a single cylinder in cross flow to air. Other works that researched the influence of roughness on lift and drag coefficients, velocity vectors, and pressure drop can be observed in Ref. [19]. The following are detailed descriptions of some related works. Achenbach et al. [4,10,11] performed a series of experimental works to examine the effect of surface roughness on heat transferred and flow topology around a single circular cylinder. Achenbach et al. [4] presented A two-roughness technique using sandpaper warping around the cylinder. Achenbach et al. [10,11] used regular pyramids arrangements. In their studies, the relative roughness (k_s/D) varied between 1.1×10^{-3} and 9.0×10^{-3}. The local heat transfer coefficient along with the temperature patterns inside the boundary layer were assessed to investigate the influence of the roughness on natural convection for a water flow over a vertical cylinder [13]. Their findings indicated that the surface roughness increased the local heat transfer rate for water. Studies [8,12] are aimed to research the impact of (k_s/D) on the convective heat transfer coefficient. Kolar [12] argued that increasing the tube roughness minimized the mean velocity and increased the friction factor as well as the heat transferred coefficient when compared to the smooth surface. Al-Rubaiy [14], carried out intensive literature survey to investigate the singular and common effects of (k_s/D) varied from 0 to 0.00725, and turbulent intensity varied between 2.2% and 9.7%, on the boundary layers around a circular cylinder. The outcomes showed that surface roughness played an essential role in augmenting thermal performance. Arenales et al. [6] analyzed experimentally the impacts of changing the surface roughness between 0.032 and 0.544 μm on copper tubes in water boiling. The findings illustrated that the rough tubes augment the heat transfer coefficient by a factor of 1.5 as compared to smooth ones. Kawamura and Takami [15] studied numerically the incompressible flow past a circular cylinder of (ε/D = 0.5%). The Reynolds numbers ranged from 1,000 to 100,000; no turbulence model was utilized. A deep reduction of drag coefficient was attained at about Re = 20,000. This indicated the capturing of the critical Reynolds number over their computational ranges. Rodrguez et al. [18] performed a Computational Fluid Dynamics (CFD) study using LES for fluid flow over rough cylinder at Re = 420,000 and equivalent sand-grain surface roughness (k_s = 0.02D). The results demonstrated that surface roughness yields a changeover to turbulence in the boundary layer. This causes flow separation produced by the enhanced drag of about 275 %when compared to the smooth cylinder.

Another option to enhance heat transfer within across flow heat exchanger, is by attaching splitter plates (SPs) at the trailing edge of the tubes as an extended surface. Such SPs addition helps much the enhancement of the heat transferred besides, reduces the greater pressure drop associated with cross flow heat exchangers due to suppression of the vortex shedding [20]. In their study, Apelt et al. [21] showed that installing SPs to circular cylinders causes the drag to decrease regardless of the Reynolds number. Kwon and Choi [22] presented a CFD work to study the influence of SPs length on vortex shedding and showed the SP critical length needed to eliminate the shedding. Another CFD work was done by Park et al. [23] on the square cylinder, and the results indicated that the shorter SP controlled the cylinder downstream wake. Mangrulkar et al. [24] involved experimental and CFD works on the effect of installing SP to a staggered tube bank in cross flow with air. The studied range of Re_{max} was (5500–14,500) and for SP with tube length to tube diameter ratio as one. The results showed that the facility of SP increased the Nusselt number for the fluid flow with the reduction in the pressure drop. Later, Mangrulkar et al. [25] presented another work to study different SPs geometries. It is found that the SP with L/D = 1.0 and t/D = 0.20 enhanced the Nusselt number and reduced the total pressure drop for most of patterns. Elmekawy et al. [26] expanded the study of Mangrulkar et al. [24] numerically to include the optimization of the SP thickness. Their results revealed that the SPs should have thin thickness to preserve optimum heat exchanger performance.

According to the literature discussion, it could be concluded that available CFD works are discussing the effect of surface roughness based on flow past a single cylinder. And there is a lack of information about the effect of surface roughness on tube bank in cross flow with air on the heat transfer and pressure drop. Hence, the idea from the present work was established to conduct a CFD study on a full 3 d model of a staggered tube bank in cross flow with air without using any symmetrical boundary conditions. As modeling the problem as it is found in reality, would give more details that can be useful. The study involves the effect of applying different surface roughness,

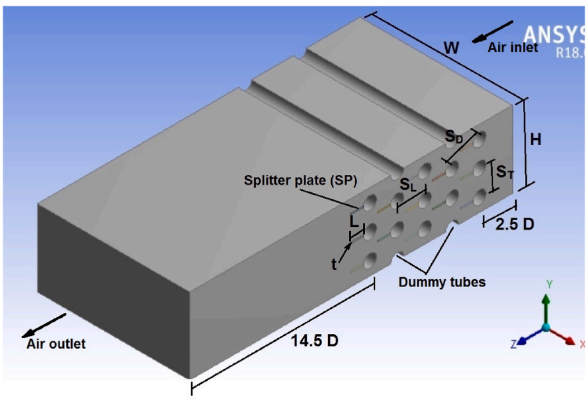

Fig. 1. Computational domain for the case of with SPs, photo from DesignModeler.

comparing results for two cases; without SPs and with SPs, and for a wide range of Re_{max}. That gives potential to the present study, however experimental validation is required.

2. CFD methodology

2.1. CFD domains and geometrical parameters

The present CFD work is a staggered bank of tubes in cross flow with air. The dimensions are taken from Incropera et al. [1], as it is found suitable for use in many applications. Where, the tube diameter (D) is 16.4 mm, the longitudinal pitch (S_L) is 34.3 mm, the transversal pitch (S_T) is 31.3 mm, and the diagonal pitch (S_D) is 37.7 mm. Thirteen tubes are considered inside the computational domain, so that, the air duct height (H) is found to be 95.4 mm, and the tube length that is equal to the air duct width is taken to be 190.8 mm (W/H = 2). For the case of splitter plates, 13 rectangular SPs are fastened to the trailing edge of each tube, the length of the SP is taken equal to the tube diameter ($L_{SP}/D = 1$), while the thickness is taken as 1.75 mm 4 half dummy tubes are added to the model to keep the flow characteristics for the staggered arrangement. A distance of 2D is considered in front of the first tube row, and a distance of 14D is considered from the last tube row to the end of the computational domain. Fig. 1, displays the geometrical parameters of the computational domain for the case of SPs, using Ansys DesignModeler R18.0, while Table 1, lists their descriptions and values.

2.2. Mesh description

A 3 d uniform volume mesh is created employing ANSYS-ICEM Mesh R18.0 per each of the two computational domains; the air domain and splitter plates domain with different cell sizes, as will be described in the mesh independency study section. Each domain meshes are of tetrahedron elements, that proved to improve the solution converges [26]. However, in such CFD problems, special attention should be considered to the boundary layer regions near both tubes and splitter plates' surfaces. Therefore, inflation has been created in such regions, using 18 layers with a first layer thickness of 0.08 mm and an inflation rate of 1.1. That assured lower Y^+ values for all studied cases. Fig. 2, is showing the generated mesh for both the air domain and splitter plate domain, for the case of SPs, (a) global view, and (b) zoom-in view to show the inflation layers.

2.3. Numerical methods and boundary conditions

This study is employing ANSYS-CFX R18.0 CFD solver code. For the case of tubes with SPs, 2 domains are identified: air as the fluid domain, and aluminum for SPs. The fluid domain boundary conditions are: fluid inlet velocity which enters from the right of the model and corresponds to Re_{max} values of 5,000, 10,000, 20,000, 50,000, 70,000, and 100,000, at a constant inlet air temperature of 288 K, pressure outlet (0 bar) at the left of the model, and hot tubes surface as walls of no-slip condition with specified roughness that changes form; smooth ($k_s/D = 0$), rough ($k_s/D = 0.01$), and rough ($k_s/D = 0.02$), and of 363 K surface temperature. The SPs domain boundary conditions are: SP bases (SPs adjoining surfaces with tubes) that are 363 K and interface with air at specified surface roughness as for the hot tube surfaces. All other walls are considered adiabatic walls. The solution convergence criterion was residual mean square type (RMS) at a residual target of 10^{-6} and lower. The turbulence model RNG k–ε is applied within the current study, as it was recommended by previous research [24,26–31]. Therefore, the solution method employed in the present study is established on the Reynolds average Navier-Stokes equations (RANS) and using RNG k–ε turbulence model. The model involved the basic mass, momentum, and energy transport equations, that can be descried for incompressible, single phase, fully developed fluid flow conditions as follows [24,26,32,33]:

Continuity equation

$$\frac{\partial \rho}{\partial t} + \frac{\partial}{\partial x_j}\left(\rho u_j\right) = 0 \quad (j = 1, 2, 3) \tag{1}$$

Momentum equation

$$\frac{\partial}{\partial t}\left(\rho\, u_j\right) + \frac{\partial}{\partial x_j}\left(\rho\, u_i\, u_j\right) = -\frac{\partial p}{\partial x_i} + \frac{\partial}{\partial x_j}\left[\mu\left(\frac{\partial u_i}{\partial x_j} + \frac{\partial u_j}{\partial x_i}\right)\right] + \frac{\partial}{\partial x_j}\left(-\rho \overline{u_i' u_j'}\right) \ (i, j = 1, 2, 3;\ \ i \neq j) \tag{2}$$

Energy equation

Table 1
Geometrical parameters specifications.

Dimension	Description	Value (mm)
D	Tubes diameter	16.4
W	Duct width	190.8
H	Duct height	95.4
S_T	Transversal pitch	31.3
S_L	Longitudinal pitch	34.3
S_D	Diagonal pitch	37.7
L_{SP}	Splitter plate length	16.4
t_{SP}	Splitter plate thickness	1.75

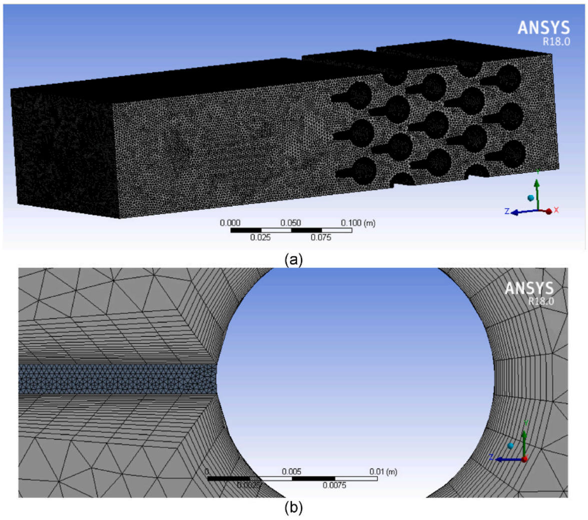

Fig. 2. Sample mesh generation (air domain and SPs domain) using Ansys-ICEM R18.0 (a) global view (b) zoom in view.

$$\frac{\partial}{\partial t}(\rho\, T)+\frac{\partial}{\partial x_j}(\rho\, u_j\, T)=\frac{\partial}{\partial x_j}\left(\frac{\mu}{\Pr}\frac{\partial T}{\partial x_j}-\rho\overline{T'\, u_j'}\right)\quad (j=1,2,3) \tag{3}$$

The terms $-\rho\overline{u_i'\, u_j'}$ and $-\rho\overline{T'\, u_j'}$ is known as Reynolds stresses and the turbulent heat flux, respectively, representing the effect of turbulence. For the RNG k–ε two equations turbulence model, the Boussinesq theory is utilized to relate the turbulent terms to that of the mean velocity and temperature as.

$$-\rho\overline{u_i'\, u_j'}=\mu_t\left(\frac{\partial u_i}{\partial x_j}+\frac{\partial u_j}{\partial x_i}\right)-\frac{2}{3}\rho\, k\,\delta_{ij}\ \ and-\rho\overline{T'\, u_j'}=\frac{\mu_t}{\Pr_t}\left(\frac{\partial T}{\partial x_j}\right) \tag{4}$$

Where μ_t is turbulence viscosity, k is TKE, δ_{ij} is kronecker delta, $\delta_{ij}=1$ (if $i=j$) and $\delta_{ij}=0$ (if $i\neq j$).

Two additional equations for the TKE, k, and the turbulence dissipation rate, ε, are solved as shown in the following.

$$\frac{\partial}{\partial t}(\rho\, k)+\frac{\partial}{\partial x_j}(\rho\, k\, u_j)=\frac{\partial}{\partial x_j}\left[\alpha_k\mu_{eff}\frac{\partial k}{\partial x_j}\right]+G_k+G_b-\rho\varepsilon\quad (i,j=1,2,3) \tag{5}$$

$$\frac{\partial}{\partial t}(\rho\,\varepsilon)+\frac{\partial}{\partial x_j}(\rho\,\varepsilon\, u_j)=\frac{\partial}{\partial x_j}\left[\alpha_\varepsilon\mu_{eff}\frac{\partial \varepsilon}{\partial x_j}\right]+C_{1\varepsilon}\frac{\varepsilon}{k}(G_k+C_{3\varepsilon}G_b)-C_{2\varepsilon}\rho\frac{(\varepsilon)^2}{k}-R_\varepsilon\ (i,j=1,2,3) \tag{6}$$

Where $C_{1\varepsilon}$, $C_{2\varepsilon}$ and $C_{3\varepsilon}$ are constants.

2.4. Equationing

The Reynolds number established on the maximum fluid velocity can be computed from Eq. (7) [34],

$$\mathrm{Re}_{max}=\frac{\rho\, \mathrm{v}_{max}\, D}{\mu} \tag{7}$$

D is the tube diameter, and ρ, and μ are the fluid density and dynamic viscosity coefficient, respectively. The upstream air mean velocity v_∞ (inlet model boundary condition) as a function of the maximum fluid velocity (v_{max}), as presented in Eq. (8),

$$\mathrm{v}_{max}=\left(\frac{S_T}{S_T-D}\right)\mathrm{v}_\infty\quad at\ S_D\ >\ \frac{S_T+D}{2} \tag{8}$$

S_T is the tubes banks transversal pitch, and S_D is the tube banks diagonal pitch. The total heat transfer rate that is added to the air (Q_a) could be calculated from Eq. (9),

$$Q_a=\dot{m}_a c_p\left(T_{a,o}T_{a,i}\right) \tag{9}$$

$\dot{m}_a$ is the air mass flow rate (calculated from Eq. (10)), c_p is the air specific heat coefficient at constant pressure, $T_{a,o}$ is the air outlet air temperature (calculated from CFD results), and $T_{a,i}$ is the air inlet temperature (kept constant at 288 K).

$$\dot{m}_a=\rho HW\mathrm{v}_\infty \tag{10}$$

Where H is the air duct height and W is the air duct width. Hence, the average convection heat transfer coefficient (h_{avg}) could be taken from Eq. (11),

$$h_{avg} = \frac{Q_a}{A_s \ \Delta T_{lm}} \tag{11}$$

where, A_s is the total heat transfer surface area, and ΔT_{lm} is the logarithmic mean temperature difference, that is computed from Eq. (12),

$$\Delta T_{lm} = \frac{(T_s - T_{a,i}) - (T_s - T_{a,o})}{\ln\left[\frac{(T_s - T_{a,i})}{(T_s - T_{a,o})}\right]} \tag{12}$$

where, T_s is the hot surface temperature (kept constant at 363 K). And the average Nusselt number could be obtained from Eq. (13),

$$Nu_{avg} = \frac{h_{avg} \ D}{K} \tag{13}$$

where, K is the air thermal conductivity. All fluid properties are evaluated at the air inlet temperature [1].

The total pressure drop could be determined from Eq. (14),

$$\Delta p = p_{a,i} - p_{a,o} \tag{14}$$

where, $p_{a,i}$ is the air static pressure at the inlet, and $p_{a,o}$ is the air static pressure at the outlet. Table 2 is summarizing the simulation studied parameters.

2.5. Mesh independency study

A mesh independence study is accomplished utilizing different seven grids. Different cells sizes have been tested for both air domain and splitter plates domain, as listed in Table 3. According to the aforementioned numerical methods, the average Nusselt number is calculated and taken as the criterion for comparison between different grids for the case of with SPs, smooth, at $Re_{max} = 5000$. It is found over the tested cases, that the air domain cells size is much influencing the *Nu* value. The value of *Nu* was found to be with little change for grids 5, 6, and 7. So, it is suggested to use grid 6 of 5,312,784 cells in the existing work. The overall mesh quality was maintained with target skewness of 0.9. All mesh independency study parameters are presented in Table 3.

2.6. CFD validation

As discussed before, there are rare available experimental data from literature studying the effect of surface roughness as found in the current study. This gives the potential to carry on experimental work in the future for the validation of the present study. However, the model is validated for the base case with the available empirical correlation of Zukauskas found in Incropera et al. [1]. The validation is conducted over the whole range of studied Re_{max} as illustrated in Fig. 3. As it is shown that, the present study CFD results are matchs the results trend from Zukauskas correlation, with an average deviation of 38.5%.

3. Results and discussions

3.1. Total heat transfer rate

Fig. 4 illustrates the present work results, in terms of total heat transfer rate (Q_a) as a function of Re_{max}. It is observed from Fig. 4 for all studied cases the rising trend of the total heat transferred as the Re_{max} increases. While the outlet air temperature showed a decay trend corresponding to the rise in the air mass flow rate. As an example, for the case without SPs and smooth surfaces (base case), the total heat transfer rate added to the air is reporting an increase of 863.23% for a change in the Re_{max} from 5000 to 100,000. Also, it is clear from Fig. 4, that installing SPs as extended surfaces helps to enhance the heat transferred rate by about 35.51% to the base case over the investigated range of Re_{max}. Now we discuss the main issue from the present study, which is increasing the heat transfer surface's roughness. It is confirmed from Fig. 4 that roughening the heat transfer surfaces enhances the total heat transfer rate. As revealed in Fig. 4, increasing the heat transfer surfaces roughness from smooth to rough ($k_s/D = 0.01$) for the base case (without SPs),

Table 2
Simulation studied parameters.

Re_{max}	Tubes surface relative roughness (k_s/D)					
	without SPs			with SPs		
5000 10,000 20,000 50,000 70,000 100,000	0.0	0.01	0.02 (Base case)	0.0	0.01	0.02

K_s - surface roughness height (mm), D - tubes diameter (16.4 mm), SPs - splitter plates.

Table 3
Mesh independency study (with SPs, smooth, $Re_{max} = 5000$).

	Mesh cells size (mm)		Total number of cells	Average Nusselt number (Nu_{avg})
	air domain	SPs domain		
Grid 1	5	0.4	2,224,900	16.611
Grid 2	4	0.35	3,307,639	16.969
Grid 3	5	0.3	4,664,005	16.611
Grid 4	4	0.3	4,840,972	16.955
Grid 5	3.5	0.3	4,991,708	17.100
Grid 6	3	0.3	5,312,784	17.320
Grid 7	2	0.3	6,656,450	17.540

SPs - splitter plates.

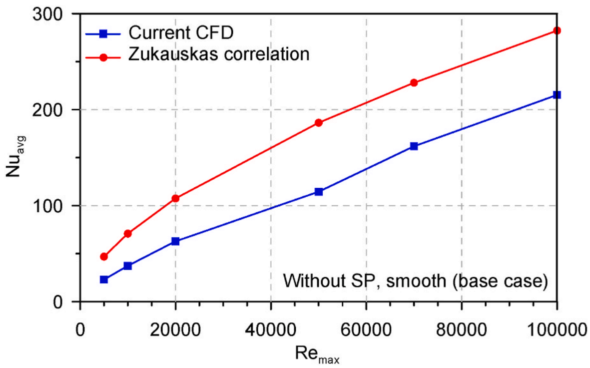

Fig. 3. Model validation for the base case.

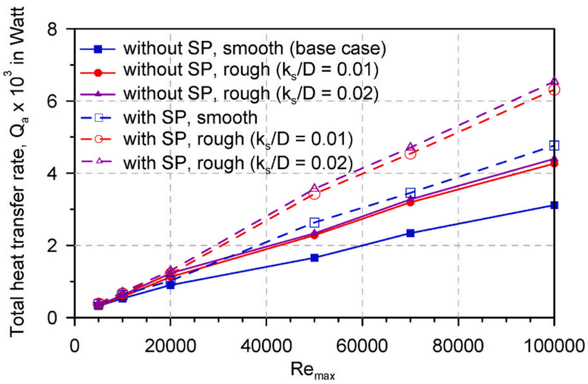

Fig. 4. Total heat transfer rate variation with Re_{max} for all studied cases.

helps to augment the total heat transfer rate by about 35.76%. However, little change can be reported when increasing the roughness from ($k_s/D = 0.01$) to ($k_s/D = 0.02$). Combining the effect of both; roughening the heat transfer surfaces, and adding SPs, led to magnifying the total heat transfer rate. It is observed from Fig. 4 that, increasing the heat transfer surface roughness from smooth to rough ($k_s/D = 0.02$) besides adding SPs yields the highest augmentation in the total heat transfer rate over the investigated range of studied parameters by about 80.56%. It is worth mentioning that the enhancement in the total heat transfer rate is positively little influenced by increasing the roughness rather than adding splitter plates in the range of Re_{max} less than about 20,000. However, a discussion based on the total pressure drop is essentially needed as will be in the next section.

3.2. Total pressure drop of tube bank

The total tube bank pressure drop is expressed in Eq. (14). Fig. 5 illustrates the resulted pressure drop for all studied cases as a function of Re_{max}. Fig. 5 demonstrated that, boosting the air mass flow rate is the main point for increasing the total tube bank pressure drop, which is consistent with the physical interpretations, resulting in higher pumping power required. As an example, for the case without SPs and smooth surfaces (base case), the total pressure drop is dramatically increased by about 58745.37% for an increase in the Re_{max} from 5000 to 100,000. While adding splitter plates as extended surfaces to the trailing edges of tubes helps to lower the total

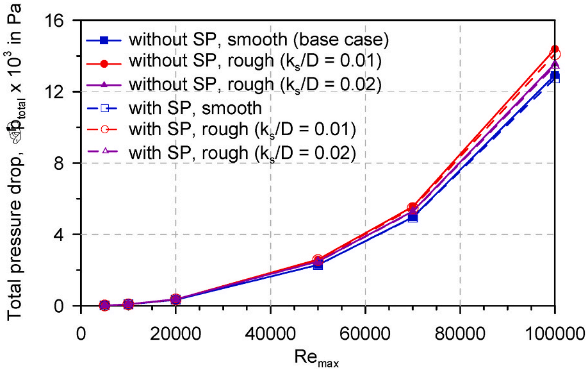

Fig. 5. Total pressure drop variation as a function of Re_{max} for all studied cases.

pressure drop of such heat exchanger, the same conclusion was found by previous works [24,26]. One could mention that adding SPs to the base case, helps to lower the total pressure drop by about 2.13% over the investigated range of Re_{max}. On contrary, it is found that increasing the heat transfer surface roughness yields a rise in the total pressure drop. As is shown in Fig. 5, roughening the heat transfer surfaces of the base case (without SPs) from smooth to rough ($k_s/D = 0.01$), and rough ($k_s/D = 0.02$), yields to increase in the total pressure drop by about 10.14%, and 2.8, respectively. This gives a positive indication about using the higher roughness ($k_s/D = 0.02$) than the lower roughness ($k_s/D = 0.01$) with comparable enhancement amounts of the total heat transfer rate.

3.3. Streamlines, velocity vectors and TKE

Fig. 6 demonstrates the flow streamlines and velocity vectors for selected cases at $Re_{max} = 50,000$: (a) without SPs and smooth (base case), (b) with SPs and smooth, (c) with SPs and rough ($k_s/D = 0.01$), and (d) with SPs and rough ($k_s/D = 0.02$). The flow topology of case (a) can be described as follows; the upstream flow is colliding with the first row of tubes resulting in stagnation patterns in front of tubes. Then the flow streamlines are moving nearby the tube walls. After that, the separation is pronounced due to the curvature of the tube circumference and a vortex area is generated behind the tubes. The streamlines from the tube above and lower sides are cooperating at the same time building a low-velocity wake recirculation region. For the subsequent tube rows, greater velocity zones are expected of longer wake zones till the last row. Fig. 6 (b) shows the effect of attaching SPs to the tubes on the flow topology. Similar flow characteristics in the upstream area are observed for the tubes with installed SPs. However, in the downstream region, installing SPs changes the flow topology. As the SPs eliminate the vortex formations from the upper and lower tubes sides. The flow streamlines

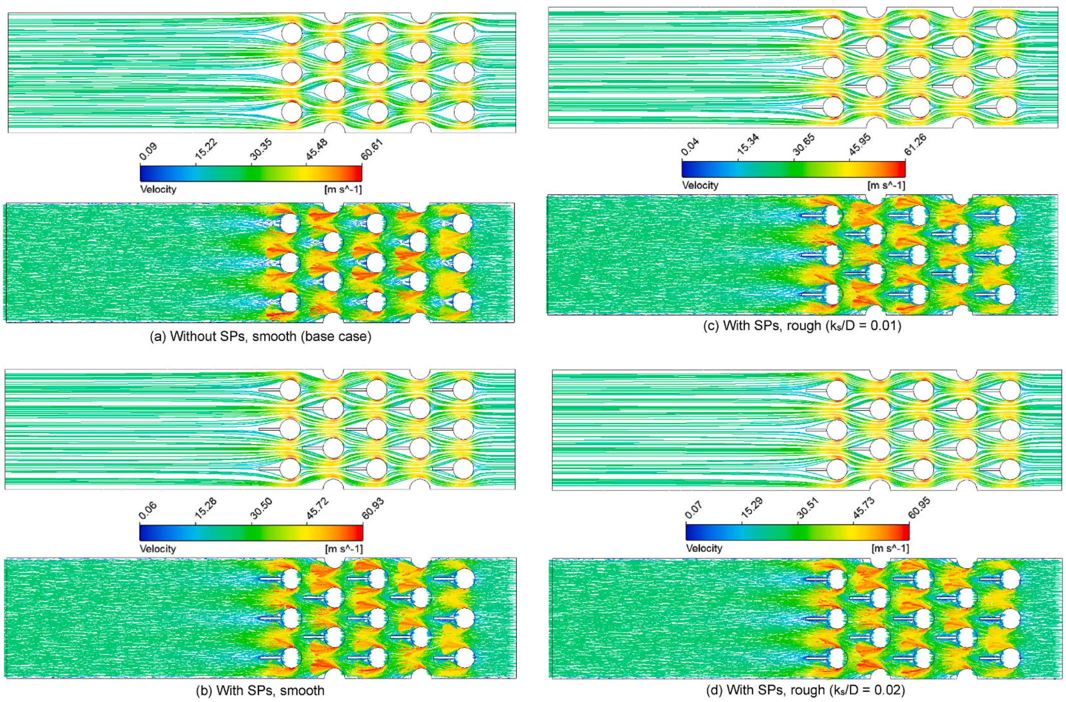

Fig. 6. Streamlines and velocity vectors for selected cases at $Re_{max} = 50,000$.

reattaching the SPs surfaces from mutually tubes sides. Yields to stratified flow that has lesser vortex strength for tubes with SPs. That would be affecting to reduce the total tube bank pressure drop (this is already proved in the total tube bank pressure drop section), and energy losses. Such flow topology is like that found by other researchers [24,26], with the novelty of this present work to be a full 3 d simulation without using any symmetrical boundaries. The impact of increasing the surface's roughness on the flow topology can be found in Fig. 6 (c) and (d). It is generally having the same main flow topology characteristics as of the smooth case (b), while differences can be drawn from the discussion based on the turbulent kinetic energy (TKE) in the coming section.

TKE can be defined as the measuring of turbulence strength in the fluid flow [32]. Therefore, it is important to examine the TKE distribution in the flow field to investigate the effect of the studied parameters: attaching SPs and increasing the surface's roughness on the intensity of eddies and vortex generation. Fig. 7 shows the TKE distribution in the flow field for all selected cases at $Re_{max} = 50{,}000$. Generally, it could be noticed from Fig. 7 that, for all presented cases, the TKE intensity increases gradually across the stream-wise direction and reaches its highest intensity downstream of the last row. The effect of installing SPs on the TKE can be observed when comparing Fig. 7 (b) to Fig. 7 (a), as lower turbulent intensity is reported for the tubes with SPs compared with those of base case (without SPs). This is mainly related to the capability of SPs to avoid the interference among the vortices from upper and lower tube sides, showing further stratified flow that characterized by little eddies and vortex growth and intensity. While increasing the surface roughness yields in significantly increase turbulent kinetic energy values as found from Fig. 7 (c) and (d). One could mention that the turbulent kinetic values for the case (d) rough ($k_s/D = 0.02$) are lower than that of lower roughness (c) rough ($k_s/D = 0.01$), and this explains the lower pressure drop reported for the higher rough ($k_s/D = 0.02$).

3.4. Temperature contours

As discussed previously in the total heat transfer section that, the change in the total heat transferred along with the growth in the Re_{max} is due to the rise in the upstream mass flow rate without significant effect from the downstream air temperature (Eq. (9)). However, at a specific Re_{max}, when comparing the different studied cases; from base case (without SPs and smooth) to the installing SPs and different surface roughness cases, the temperature variations is the main parameter that influencing the total heat transfer enhancement (Eq. (9)). Therefore, it was of importance to show temperature contours from the present CFD study for different cases using high number of contours for better image resolution. Fig. 8 depicts temperature contours for selected cases at $Re_{max} = 50{,}000$, the images are generated using 100 number of contours. One could notice from the images that, there is a gradual increase in the downstream air temperature from the base case (a) without SPs and smooth (base case), then case (b) with SPs and smooth, then case (c) with SPs and rough ($k_s/D = 0.01$), and to case (d) with SPs and rough ($k_s/D = 0.02$). This gradual increase in the downstream air temperature can be observed by following the high intensity of the light blue color rather than the dim blue one. Such an increase in the downstream air temperature directly increases the temperature difference found in Eq. (9), which is the main reason for the total heat transferred enhancement.

4. Conclusions

A full 3 d CFD model without any symmetrical boundary conditions is investigated to study the heat transferred and total pressure drop for tube bank of staggered arrangement in cross flow with air. Two options of heat transfer enhancement; attaching splitter plates to the trailing edge of the tubes and increasing the heat transfer surface roughness are studied. The tube bank is of 13 tubes, 16.4 mm tubes diameter, 34.3 mm longitudinal pitch, 31.3 mm transversal pitch, and 37.7 mm diagonal pitch. The length of the SP is taken as equal to the tube diameter ($L_{SP}/D = 1$), while the thickness is taken as 1.75 mm. Four half dummy tubes are added to the model to keep the flow characteristics for the staggered arrangement. The study extended to include the effect of Re_{max} changes from 5000 to 100,000. While three surface relative roughness; $k_s/D = 0$, $k_s/D = 0.01$, and $k_s/D = 0.02$ are investigated. The results indicated that the total heat transferred increases as the Re_{max} increases. While the outlet air temperature showed a decay trend corresponding to the increase in the air mass flow rate. As an example, for the case without SPs and smooth surfaces (base case), the total heat transfer rate added to the air is reporting an increase of 863.23% for a change in the Re_{max} from 5000 to 100,000. Also, installing SPs as extended surfaces helps to enhance the heat transferred rate by about 35.51% to the base case over the investigated range of Re_{max}. The results confirmed that increasing heat transfer surface roughness helps to augment the total heat transferred. While limited pressure drop increase is reported compared to installing SPs. As it was detected that, rising the heat transfer surface roughness from smooth, ($k_s/D = 0$) to rough, ($k_s/D = 0.01$) for the case (without SPs), helps to augment the total heat transfer rate by about 35.76%. However, little change can be reported when increasing the roughness from ($k_s/D = 0.01$) to ($k_s/D = 0.02$). Combining the effect of both; roughening the heat transfer surfaces, and adding SPs, led to multiplying the total heat transfer rate. As by changing the surface roughness from smooth to rough ($k_s/D = 0.02$) besides adding SPs yields the highest augmentation in the total heat transfer rate over the investigated range of studied parameters by about 80.56%. It is worth mentioning that the enhancement in the total heat transfer rate is positively little influenced by increasing the roughness rather than adding splitter plates in the range of Re_{max} less than about 20,000.

Credit author statement

Mohamed A. Karali: Management and coordination responsibility for the research activity planning and execution, Conceptualization, CFD simulation, methodology, Data collection, Writing- Original draft preparation, Manuscript preparation and data analysis. Bandar Awadh Almohammadi: Conceptualization, Writing and manuscript editing. Abdullah S. Bin Mahfouz: Conceptualization, Writing and manuscript editing. Mostafa A. H. Abdelmohimen: Conceptualization, Writing and manuscript editing. El-Awady Attia: Conceptualization, Writing and manuscript editing. H. A. Refaey: Conceptualization, Writing- Original draft preparation. Manuscript preparation and data analysis.

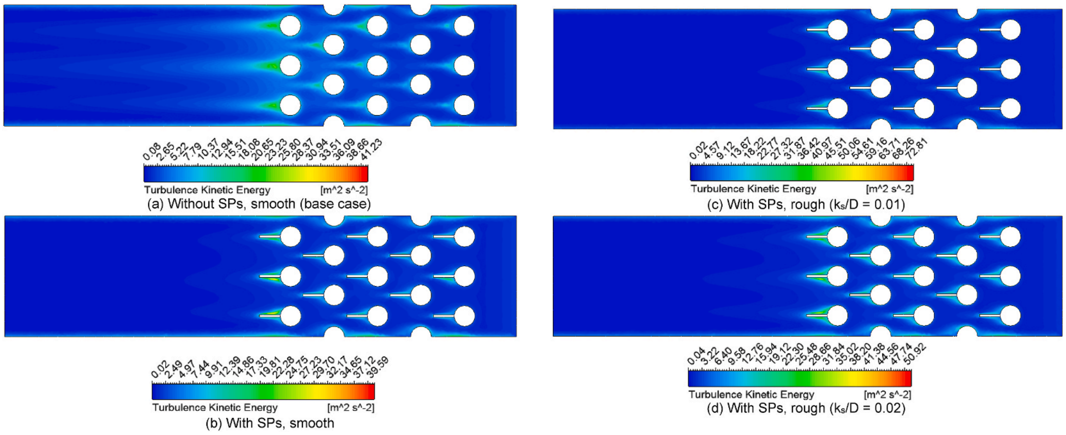

Fig. 7. Turbulent kinetic energy for selected cases at $Re_{max} = 50,000$.

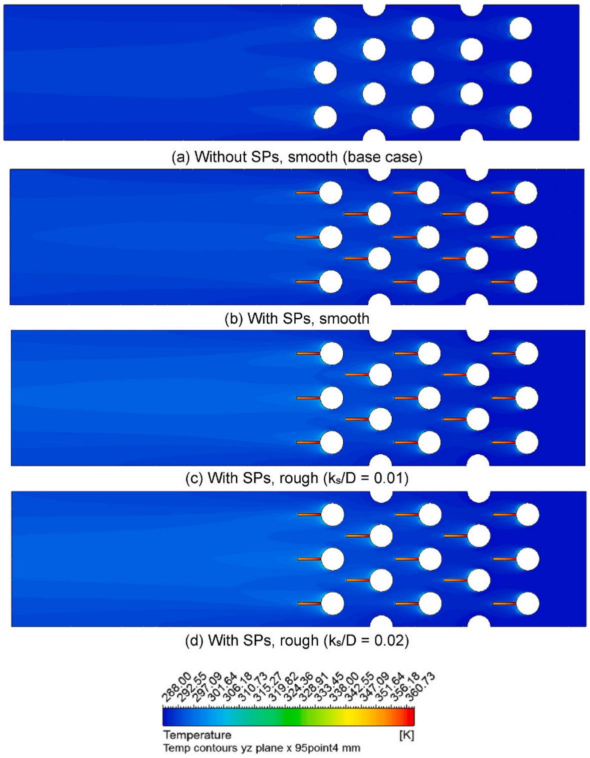

Fig. 8. Temperature contours for selected cases at $Re_{max} = 50,000$.

Declaration of competing interest

The authors declare that they have no known competing financial interests or personal relationships that could have appeared to influence the work reported in this paper.

Data availability

No data was used for the research described in the article.

References

[1] F. Incropera, P.D. Dewitt, T.L. Bergman, A.S. Lavine, in: Fundamentals of Heat and Mass Transfer, sixth ed., John Wiley & Sons Inc., 2006. Ch (7).
[2] Y.A. Cengel, Heat Transfer: a Practical Approach, MacGraw-Hill, 2003.

[3] J.P. Batham, Pressure distributions on circular cylinders at critical Reynoldsnumbers, J. Fluid Mech. 57 (1973) 209–228, 02.
[4] E. Achenbach, Influence of surface roughness on the cross-flow around a circular cylinder, J. Fluid Mech. 46 (1971) 321–335, 02.
[5] M.P. Schultz, K.A. Flack, Turbulent boundary layers over surfaces smoothed by sanding, Journal of fluid engineering 125 (5) (2003) 863–870.
[6] M.R.M. Arenales, S. Kumar, L. Kuo, P. Chen, Surface roughness variation effects on copper tubes in pool boiling of water, Int. J. Heat Mass Tran. 151 (2020), 119399, https://doi.org/10.1016/j.ijheatmasstransfer.2020.119399.
[7] D.J. Bergstrom, M.F. Tachie, R. Balachandar, Application of power laws to low Reynolds number boundary layers on smooth and rough surfaces, Phys. Fluids 13 (11) (2001) 3277–3284.
[8] V.l. Gomelauri, Influence of two-dimensional artificial roughness on convective heat transfer, Int. J. Heat Mass Tran. 7 (6) (1964) 653–663.
[9] P.A. Krogstadt, R.A. Antonia, Surface roughness effects in turbulent boundary layers, Exp. Fluid 27 (5) (1999) 450–460.
[10] E. Achenbach, The effect of surface roughness on the heat transfer from a circular cylinder to the cross flow of air, Int. J. Heat Mass Tran. 20 (1977) 359–369.
[11] E. Achenbach, E. Heinecke, On vortex shedding from smooth and rough cylinders in the range of Reynolds numbers 6 x 103 to 5 x 106, J. Fluid Mech. 109 (1981) 239–251.
[12] V. Kolár, Heat transfer in turbulent flow of fluids through smooth and rough tubes, Int. J. Heat Mass Tran. 8 (4) (1965) 639–653.
[13] F. Tetsu, F. Motoo, T. Masanori, Influence of various surface roughness on the natural convection, Int. J. Heat Mass Tran. 16 (3) (1973) 629–636.
[14] A. Al-Rubaiy, The Effect of Surface Roughness and Free Stream Turbulence on the Flow and Heat Transfer Around a Circular Cylinders, University of Sheffield, 2018. PhD dissertation.
[15] T. Kawamura, H. Takami, Computation of high Reynolds number flow around a circular cylinder with surface roughness, Fluid Dynam. Res. 1 (1986) 145–162.
[16] D. Lakehal, Computation of turbulent shear flows over rough-walled circular cylinders, J. Wind Eng. Ind. Aerod. 80 (1) (1999) 47–68.
[17] F. Dierich, P.A. Nikrityuk, A numerical study of the impact of surface roughness on heat and fluid flow past a cylindrical particle, Int. J. Therm. Sci. 65 (2013) 92–103.
[18] I. Rodrguez, O. Lehmkuhl, U. Piomelli, J. Chiva, R. Borrell, A. Oliva, Numerical simulation of roughness effects on the flow past a circular cylinder, J. Phys. Conf. 745 (2016). https://doi:10.1088/1742-6596/745/3/032043.
[19] J.B. Taylor, A.L. Carrano, S.G. Kandlikar, Characterization of the effect of surface roughness and texture on fluid flow - past, present, and future, Int. J. Therm. Sci. 45 (10) (2006) 962–968.
[20] A. Roshko, Experiments on the flow past a circular cylinder at very high Reynolds number, J. Fluid Mech. 10 (1961) 345–356, https://doi.org/10.1017/S0022112061000950.
[21] C.J. Apelt, G.S. West, A.A. Szewczyk, The effects of wake splitter plates on the flow past a circular cylinder in the range 10000<Re<50000, J. Fluid Mech. 61 (1973) 187–198, https://doi.org/10.1017/S0022112073000649.
[22] K. Kwon, H. Choi, Control of laminar vortex shedding behind a circular cylinder using splitter plates, Phys. Fluids 8 (1996) 479–486, https://doi.org/10.1063/1.868801.
[23] W.C. Park, Numerical investigation of wake flow control by a splitter plate, KSME Int. J. 12 (1998) 123–131, https://doi.org/10.1007/BF02946540.
[24] C.K. Mangrulkar, A.S. Dhoble, S.G. Chakrabarty, U.S. Wankhede, Experimental and CFD prediction of heat transfer and friction factor characteristics in cross flow tube bank with integral splitter plate, Int. J. Heat Mass Tran. 104 (2017) 964–978, https://doi.org/10.1016/j.ijheatmasstransfer.2016.09.013.
[25] C.K. Mangrulkar, A.S. Dhoble, J.D. Abraham, S. Chamoli, Experimental and numerical investigations for effect of longitudinal splitter plate configuration for thermal-hydraulic performance of staggered tube bank, Int. J. Heat Mass Tran. 161 (2020), 120280, https://doi.org/10.1016/j.ijheatmasstransfer.2020.120280.
[26] A.M.N. Elmekawy, A.A. Ibrahim, A.M. Shahin, S. Al-Ali, G.E. Hassan, Performance enhancement for tube bank staggered configuration heat exchanger – CFD Study, Chem. Eng. Process: Process Intensif. 164 (2021), 108392, https://doi.org/10.1016/j.cep.2021.108392.
[27] T.A. Ibrahim, A. Gomaa, Thermal performance criteria of elliptic tube bundle in cross flow, Int. J. Therm. Sci. 48 (2009) 2148–2158, https://doi.org/10.1016/j.ijthermalsci.2009.03.011.
[28] E. Ibrahim, M. Moawed, Forced convection and entropy generation from elliptic tubes with longitudinal fins, Energy Convers. Manag. 50 (2009) 1946–1954, https://doi.org/10.1016/j.enconman.2009.04.021.
[29] S.S.E. Ahmed, E.Z. Ibrahiem, O.M. Mesalhy, M.A. Abdelatief, Effect of attack and cone angels on air flow characteristics for staggered wing shaped tubes bundle, Heat Mass Tran./Waerme- Und Stoffuebertragung 51 (2015) 1001–1016, https://doi.org/10.1007/s00231-014-1473-3.
[30] S.S.A.E. Ahmed, O.M. Mesalhy, M.A. Abdelatief, Effect of longitudinal-external-fins on fluid flow characteristics for wing-shaped tubes bundle in cross flow, J. Therm. (2015), https://doi.org/10.1155/2015/542405, 2015.
[31] M.E. Nakhchi, J.A. Esfahani, Numerical investigation of turbulent CuO–water nanofluid inside heat exchanger enhanced with double V-cut twisted tapes, J. Therm. Anal. Calorim. (2020), https://doi.org/10.1007/s10973-020-09788-4.
[32] D.C. Wilcox, Turbulence Modelling for CFD, third ed.ftion, DCW Industries, Inc., 2006.
[33] G.D. Stefanidis, B. Merci, G.J. Heynderickx, G.B. Marin, CFD simulations of steam cracking furnaces using detailed combustion mechanisms, Comput. Chem. Eng. 30 (2006) 635–649, https://doi.org/10.1016/j.compchemeng.2005.11.010.
[34] H.A. Refaey, A.M. Sultan, M. Moawad, M.A. Abdelrahman, Numerical investigations of the convective heat transfer from turbulent flow over staggered tube bank, J. Inst. Eng. India Ser. C 100 (6) (2019) 983–993, https://doi.org/10.1007/s40032-018-0493-z.